Thermochimica Acta, 156 (1989) 137–145
Elsevier Science Publishers B.V., Amsterdam – Printed in The Netherlands

THE KINETICS OF THE THERMALLY INDUCED ISOMERIZATION OF SOME NICKEL(II) COMPLEXES CONTAINING BUTANEDIAMINES IN A SOLID PHASE

YOSHIO MASUDA

General Education Department, Niigata University, Niigata 950-21 (Japan)

TAKASHI MATSUDA

Department of Chemistry, Faculty of Science, Niigata University, Niigata 950-21 (Japan)

HIROSHI KUME

Course of Fundamental Science and Technology, Graduate School of Science and Technology, Niigata University, Niigata 950-21 (Japan)

YOSHINORI IHARA

Department of Chemical Science, Division of Physical Sciences, Graduate School of Natural Science and Technology, Kanazawa University, Kanazawa 920 (Japan)

(Received 18 April 1989)

ABSTRACT

The nickel(II) complexes, $[Ni(1,2\text{-bn})_2]X_2$ and $[Ni(m\text{-bn})_2](NO_3)_2$, where 1,2-bn and *m*-bn are 1,2-butanediamine and *meso*-2,3-butanediamine, respectively, and X is Cl^- or Br^-, are thermally isomerized from a square planar to an octahedral structure by anation of counter ions in the solid phase. The kinetics of the isomerization was studied on the basis of the results of differential scanning calorimetry.

The isomerizations of 1,2-bn complexes with Cl^- and Br^- are considered to be first-order reactions (F_1). The activation energies for the isomerizations of chloride and bromide complexes were 227 ± 4 and 214 ± 10 kJ mol^{-1}, respectively. The isomerization of *m*-bn complex with NO_3^- proceeded as an Avrami–Erofe'ev-type reaction (A_2), and the activation energy was 321 ± 10 kJ mol^{-1}.

INTRODUCTION

It is well-known that the nickel(II) ion forms complexes of various coordination structures [1], e.g. octahedral, tetrahedral and square planar, depending on the ligand, and that mutual transformation often occurs among these structures. For example, it has been shown recently that the solid complexes of $[Ni(1,2\text{-bn})_2]X_2$ (1,2-bn ≡ 1,2-butanediamine and X ≡

0040-6031/89/$03.50

Cl^- or Br^-) and $[Ni(m\text{-bn})_2](NO_3)_2$ (*m*-bn ≡ *meso*-2,3-butanediamine) were thermally isomerized from a square planar (Sp) to an octahedral (Oh) structure by anation of counter ions [1–4].

Although it is interesting to investigate the mechanism of the isomerizations occurring in a solid state, such a study has scarcely been reported. A kinetic investigation on the basis of a thermal analysis is an effective method of clarifying the mechanism of a solid-state reaction. When a solid reaction such as thermal dehydration and decomposition is accompanied by a weight change, thermogravimetry (TG) is suitable for the kinetic analysis of the reaction. On the other hand, differential scanning calorimetry (DSC) is useful for the kinetic analysis of a reaction, such as the present isomerization, which is not accompanied by a weight change.

We have recently analysed the kinetics of thermal dehydration of some inorganic hydrates using a microcomputer to acquire and process the large amount of precise data required for thermal analysis [5–7]. In this study, the method is used to analyse the thermal isomerizations of $[Ni(1,2\text{-bn})_2]X_2$ ($X \equiv Cl^-$ or Br^-) and $[Ni(m\text{-bn})_2](NO_3)_2$.

EXPERIMENTAL

Preparation of compounds

The ligands 1,2-bn and *m*-bn, and their complexes *trans*-$[Ni(H_2O)_2(1,2\text{-bn})_2]X_2$ and $[Ni(m\text{-bn})_2](NO_3)_2$, were obtained using methods described in the literature [4,8–10]. The results of elemental analyses are shown in Table 1.

Apparatus

TG and differential thermal analysis (DTA) were performed on a Rigaku Thermoflex TG-DTA M 8075 apparatus. DSC measurements were made with a Shinku Richo DSC-1500 M5/L. Figure 1 shows a block diagram of

TABLE 1

Elemental analyses of the complexes

Complexes	Analytical data [a]		
	H(%)	C(%)	N(%)
trans-$[Ni(H_2O)_2(1,2\text{-bn})_2]Cl_2$	8.43 (8.25)	27.65 (28.10)	16.12 (16.38)
trans-$[Ni(H_2O)_2(1,2\text{-bn})_2]Br_2$	6.68 (6.55)	21.97 (22.30)	12.58 (13.00)
$[Ni(m\text{-bn})_2](NO_3)_2$	26.46 (26.76)	6.82 (6.74)	23.21 (23.41)

[a] Calculated values are in parentheses.

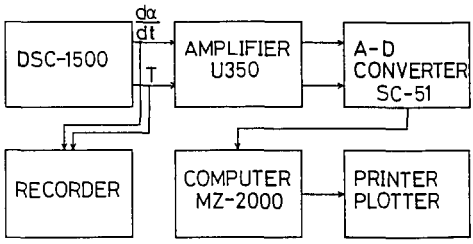

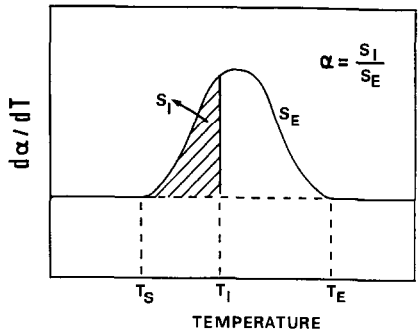

Fig. 1. Block diagram of experimental system for DSC measurements.

Fig. 2. Determination of fraction of reaction (α) from DSC curve: S_E, total area of this peak; S_I, area evolved up to temperature, T_I; T_S, temperature at which reaction starts; and T_E, temperature at which reaction ends.

the system for the DSC measurements. The DSC output voltages were amplified with a UNIPULSE U350A amplifier and acquired on a microcomputer (SHARP MZ-2000) via an AD converter (THINKY SC-51). A printer (EPSON RP-80) and an x–y plotter (GRAPHTEC MP2000) were connected to the computer. The DSC measurements were carried out at heating rates of 4.6, 6.9, 9.3 and 11.7 K min^{-1} with α-alumina as a reference material. The DSC instrument was calibrated from the heat of fusion of indium (99.999%) ($\Delta H = 3.3$ kJ mol^{-1} at 430 K) [11]. For each measurement, 5–8 mg of specimen were weighed into an aluminium crucible and about 3000 data points concerning the isomerization were collected at regular time intervals.

The X-ray diffraction profile of a powder specimen was taken with nickel-filtered Cu $K\alpha$ radiation on a Rigaku Rado-B diffractometer.

IR spectra were measured from 250 to 4000 cm^{-1} in KBr disks on a Hitachi 295 spectrophotometer.

Solid-phase electronic spectra in the visible range were measured with a Hitachi U-3200 spectrophotometer equipped with a head-on photomultiplier (150-0903). The spectra at elevated temperatures were obtained using a handmade heating block.

Kinetic analysis

The rate of a solid-state reaction is expressed by

$$d\alpha/dt = k\,F(\alpha) \tag{1}$$

where α is the fraction of reaction after time t, $F(\alpha)$ is a function depending on the reaction mechanism as shown in Table 2 [12] and k is a rate constant.

TABLE 2

Commonly used $F(\alpha)$ for solid-phase reactions

$F(\alpha)$	Symbol	Rate-determining process
α^{-1}	D_1	One-dimensional diffusion
$[-\ln(1-\alpha)]^{-1}$	D_2	Two-dimensional diffusion
$[(1-\alpha)^{1/3}-1]^{-1}(1-\alpha)^{2/3}$	D_3	Three-dimensional diffusion (Jander equation)
$[(1-\alpha)^{-1/3}-1]^{-1}$	D_4	Three-dimensional diffusion (Ginstring–Brounshtein equation)
$(1-\alpha)^{1/2}$	R_2	Two-dimensional phase boundary reaction
$(1-\alpha)^{2/3}$	R_3	Three-dimensional phase boundary reaction
$(1-\alpha)$	F_1	First-order reaction
$(1-\alpha)[-\ln(1-\alpha)]^{1/2}$	A_2	Avrami–Erofe'ev equation ($n=2$)
$(1-\alpha)[-\ln(1-\alpha)]^{2/3}$	A_3	Avrami–Erofe'ev equation ($n=3$)

According to the Arrhenius equation, the rate constant is a function of the absolute temperature T

$$k = A \exp(-E/RT) \tag{2}$$

where A, E and R are the pre-exponential factor, the activation energy and the gas constant, respectively. Substituting eqn. (2) into eqn. (1) and assuming a linear heating rate ($\beta = dT/dt$) yields

$$[(d\alpha/dT)\beta] = A \exp(-E/RT)\ F(\alpha) \tag{3}$$

and the logarithmic form of eqn. (3)

$$\ln[(d\alpha/dT)\beta] - \ln\ F(\alpha) = \ln\ A - E/RT \tag{4}$$

In this study, the rate of reaction $[(d\alpha/dT)\beta]$ can be directly determined from the DSC measurements. The suitability of the $F(\alpha)$ selected for the reaction can be judged on the basis of the linearity of the plots of the left-hand side against $1/T$, in accordance with eqn. (4) (Achar's plot) [13]. The activation energy (E) can be determined from its slope and checked by the modified Friedman method described previously [5,14]. The value of A was determined by introducing the experimental values of $[(d\alpha/dT)\beta]$, E and $F(\alpha)$ into eqn. (4). The fraction of reaction (α) at a temperature T_I was derived from the ratio of the area corresponding to the heat evolved up to T_I (S_I) to the integral area for the total heat of reaction (S_E) as shown in Fig. 2.

RESULTS AND DISCUSSION

The complexes of *trans*-$[Ni(H_2O)_2(1,2\text{-bn})_2]Cl_2$ and *trans*-$[Ni(H_2O)_2(1,2\text{-bn})_2]Br_2$ were dehydrated at temperatures ranging from 60 to 90 °C

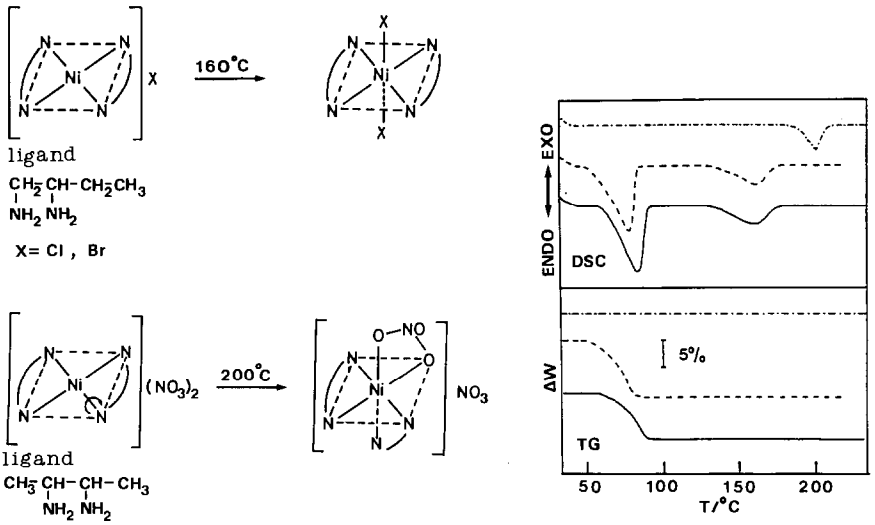

Fig. 3. Schematic expression of isomerizations of complexes.

Fig. 4. DSC and TG curves of (———) $[Ni(H_2O)_2(1,2\text{-bn})_2]Cl_2$, (- - - - -) $[Ni(H_2O)_2(1,2\text{-bn})_2]Br_2$ and (·—·—·) $[Ni(m\text{-bn})_2](NO_3)_2$.

$$trans\text{-}[Ni(H_2O)_2(1,2\text{-bn})_2]Cl_2 \rightarrow [Ni(1,2\text{-bn})_2]Cl_2 + 2H_2O \quad (a)$$

$$trans\text{-}[Ni(H_2O)_2(1,2\text{-bn})_2]Br_2 \rightarrow [Ni(1,2\text{-bn})_2]Br_2 + 2H_2O \quad (b)$$

In addition, the dehydrated complexes were isomerized from a square planar (Sp) to an octahedral structure (Oh) at temperatures ranging from 125 to 180 °C

$$[Ni(1,2\text{-bn})_2]Cl_2(Sp) \rightarrow trans\text{-}[NiCl_2(1,2\text{-bn})_2](Oh) \quad (c)$$

$$[Ni(1,2\text{-bn})_2]Br_2(Sp) \rightarrow trans\text{-}[NiBr_2(1,2\text{-bn})_2](Oh) \quad (d)$$

The complex $[Ni(m\text{-bn})_2](NO_3)_2$ was similarly isomerized at temperatures ranging from 180 to 215 °C

$$[Ni(m\text{-bn})_2](NO_3)_2(Sp) \rightarrow cis\text{-}[Ni(NO_3)(m\text{-bn})_2](NO_3)(Oh) \quad (e)$$

These reactions have been reported by Ihara et al. [2–4]. The isomerizations, (c), (d) and (e), are structural transformations as shown schematically in Fig. 3.

Figure 4 shows the DSC and TG curves for these complexes. In the DSC curves, there are two endothermic peaks at 85 and 79 °C, corresponding to dehydrations (a) and (b), respectively. After the dehydrations, endothermic peaks without weight change for isomerizations (c) and (d) are observed at

TABLE 3

$F(\alpha)$ function, activation energy (E), pre-exponential factor (A) and enthalpy change (ΔH) for the isomerization

Complex	Isomerization [a]	$F(\alpha)$	E (kJ mol^{-1})	log A (min^{-1})	ΔH (kJ mol^{-1})
$[Ni(1,2\text{-bn})_2]Cl_2$	(c)	F_1	227±4	27.2	19.8±0.90
$[Ni(1,2\text{-bn})_2]Br_2$	(d)	F_1	214±10	23.9	16.4±1.2
$[Ni(m\text{-bn})_2](NO_3)_2$	(e)	A_2	321±10	35.6	8.25±0.31

[a] See text.

temperatures ranging from 125 to 180 °C. The endothermic peak for isomerization (e) is at slightly higher temperatures, from 180 to 215 °C. In addition, before and after the endothermic reactions (c), (d) and (e), the specimens clearly changed in colour from yellow to violet-blue. The colours slowly changed from violet-blue back to yellow on cooling the specimens to room temperature.

The enthalpy change (ΔH) caused by these isomerizations shows the energy gap between the square planar and the octahedral configurations, and the values obtained from the DSC measurements are shown in Table 3. Although there is little difference in the values of ΔH between isomerizations (c) and (d), the value for isomerization (e) is nearly half those for (c) and (d). These enthalpy changes consist of a number of components, i.e. an exothermic portion due to the formation of Ni–X(X = Cl^-, Br^- or NO_3^-) bonds, and an endothermic contribution from the weakening of the four Ni–N bonds in changing from a low-spin to a high-spin state, and from other factors such as changes in lattice energy, steric repulsion, etc. However, further analysis of the ΔH value cannot be given at present because the detailed crystal structures of these complexes before and after isomerization have not been clarified.

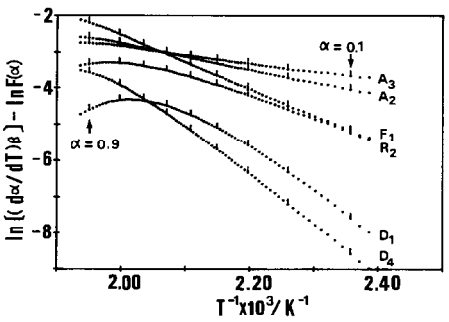

Fig. 5. Achar's plot for isomerization (e).

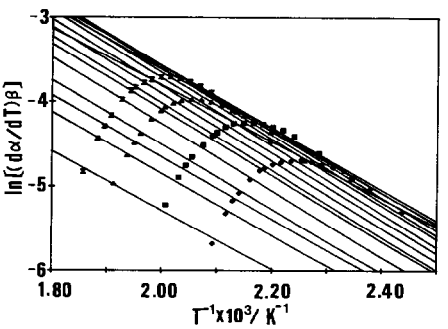

Fig. 6. Plots of $\ln[(d\alpha/dT)\beta]$ versus $1/T$ from $\alpha = 0.10$–0.90 for isomerization (e).

TABLE 4

Estimation of $F(\alpha)$ and activation energy (E) for isomerization (e) using Achar's method [a]

$F(\alpha)$	α-range [b]	E (kJ mol^{-1})	r [c]
A_3	0.08–0.92	198	0.9983
A_2	0.09–0.91	309	0.9994
F_1	0.07–0.91	152	0.9998

[a] Results from the data obtained at a heating rate of 9.3 K min^{-1}.
[b] α-range shows the region in which each reaction takes place.
[c] Correlation coefficient.

Figure 5 shows Achar's plot for isomerization (e) in accordance with eqn. (4). In the present study, we examined the plots for the nine models of $F(\alpha)$ listed in Table 2. The plots of F_1, A_2 and A_3 show the best linearity over nearly the whole reaction range. The activation energy values (E) obtained from these plots are listed in Table 4 together with their correlation coefficients. To select the most reliable of these three functions, the values of E were compared with those obtained using the modified Friedman method [5,14] for isomerization (e). Figure 6 shows modified Friedman's plots for isomerization (e). Parallel lines are apparent in the range $0.10 \leqslant \alpha \leqslant 0.90$. The mean value of E determined from the slopes of these lines was 321 ± 10 kJ mol^{-1}. This value is comparable with that, 309 kJ mol^{-1}, obtained from Achar's plot for the A_2 function in Table 4. From this fact, we confirm that the A_2 function is a reasonable model for isomerization (e).

Isomerizations (c) and (d) were also analysed kinetically by the same procedure. Both reactions were found to be first-order (F_1), as shown in Table 3. The X-ray diffractions were measured before and after isomerizations (c) and (d) for the chloride and bromide complexes, respectively. As shown in Fig. 7, their profiles are similar, i.e. (1) and (3) or (2) and (4). These findings show that both isomerizations are attributable to a similar structural change.

The activation energy of isomerization (e) is larger than those of (c) and (d), as shown in Table 3. This is consistent with the fact that isomerization (e) takes place at slightly higher temperatures than those of (c) and (d), as shown in Fig. 4. This finding seems to be attributable to the complexity of isomerization (e), in comparison with those of (c) and (d). The reflectance spectrum [2] and the IR spectrum [3,15] of the transformed complex, $Ni(NO_3)_2(m\text{-bn})_2$, indicate that the complex has an octahedral structure of *cis* form, and one of the NO_3^- coordinates as a bidentate ligand, while the other remains as an uncoordinated ion. On coordination of the NO_3^- to the *cis* positions of the square-planar complex ion $[Ni(m\text{-bn})_2]^{2+}$, at least, one chelate ring $\widehat{NNNi}$ should rotate through 90° about the Ni–N bond in the transition state, as shown in Fig. 3. On the other hand, reactions (c) and (d)

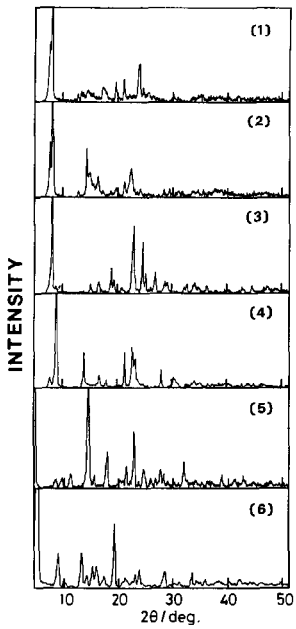

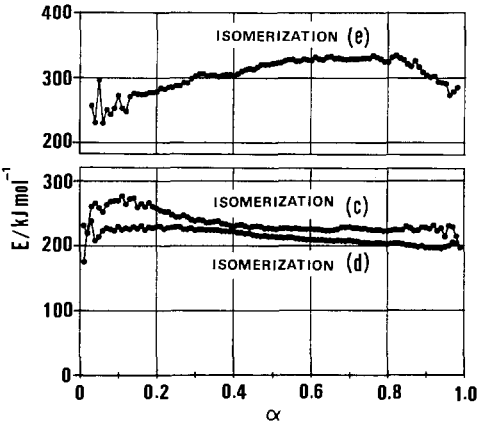

Fig. 7. X-ray powder diffraction profiles of original and isomerized complexes: (1), $[Ni(1,2\text{-}bn)_2]Cl_2$; (2), $[NiCl_2(1,2\text{-}bn)_2]$; (3), $[Ni(1,2\text{-}bn)_2]Br_2$; (4), $[NiBr_2(1,2\text{-}bn)_2]$; (5), $[Ni(m\text{-}bn)_2](NO_3)_2$; and (6), $[Ni(NO_3)(m\text{-}bn)_2](NO_3)$.

Fig. 8. Relation between activation energy (E) and fraction of isomerization (α).

involve the direct anation of Cl^- and Br^- to the *trans* positions, respectively. It is reasonable that high activation energies should be required for such a complicated reaction as (e) in comparison with the simple reactions (c) and (d).

For isomerization in such a solid phase, the process involving anation may consist of two steps, i.e. migration of the anion from the lattice site to the complex ion, and then formation of the transition state. The activation energy required for the process is expected to increase with increasing lattice energy. Because for a given cation, e.g. $[Ni(1,2\text{-}bn)_2]^{2+}$, the lattice energy is assumed to increase with a decrease in anion size, it is reasonable that the crystal of the chloride complex should have a higher lattice energy than that of the bromide complex. Therefore, the activation energy for isomerization (c) becomes higher than that of (d) [16].

Figure 8 shows the relation between the activation energy determined from the modified Friedman method and the fraction of isomerization. It is noteworthy that the values of E for the first stages of isomerizations (c) and (d) are slightly higher than those for the later main stages, whereas in isomerization (e), the value of E for the later main stages is higher than that for the earlier one. This can be explained in terms of the following reaction mechanism. With the preceding assumption that an anation in solid state

involves at least two steps, i.e. the migration of anion from a lattice site to the complex ion and the formation of a transition state, the rate-determining steps for both isomerizations (c) and (d) seem to be their initial steps and that for isomerization (e) to be the later step.

ACKNOWLEDGEMENT

The authors wish to express their thanks to Professor Yoshio Ito of Niigata University for many useful discussions. Thanks are also given to Mr. Katsumi Hirasawa for his assistance in the experimental work.

REFERENCES

1 Y. Ihara, Dr. Sci. Thesis, Kyushu University, Fukuoka, Japan, 1987.
2 Y. Ihara, T. Kamishima and R. Tsuchiya, Thermochim. Acta, 67 (1983) 23.
3 Y. Ihara, Y. Fukuda and K. Sone, Bull. Chem. Soc. Jpn., 59 (1986) 1825.
4 Y. Ihara, A. Wada, Y. Fukuda and K. Sone, Bull. Chem. Soc. Jpn., 59 (1986) 2309.
5 Y. Masuda, Y. Ito, R. Ito and K. Iwata, Thermochim. Acta, 99 (1986) 205.
6 Y. Masuda, Y. Ito, R. Ito and K. Iwata, Thermochim. Acta, 102 (1986) 263.
7 Y. Masuda, K. Iwata, R. Ito and Y. Ito, J. Phys. Chem., 91 (1987) 6543.
8 L.B. Clapp, J. Am. Chem. Soc., 70 (1948) 184.
9 H. Nishimoto, T. Yoshikuni, A. Uehara, E. Kyuno and R. Tsuchiya, Bull. Chem. Soc. Jpn., 51 (1978) 1068.
10 F.H. Dickey, W. Fickett and H.J. Lucas, J. Am. Chem. Soc., 74 (1952) 944.
11 Kagaku Binran Kisohen II (Handbook of Chemistry), The Chemical Society of Japan, Maruzen, Tokyo, 3rd edn., 1984, p. 270.
12 J.H. Sharp, G.W. Brindley and B.N.N. Achar, J. Am. Ceram. Soc., 49 (1966) 379.
13 B.N.N. Achar, G.W. Brindley and J.H. Sharp, Proc. Int. Clay Conf., Jerusalem, 1 (1966) 67.
14 H.L. Friedman, J. Polym. Sci. Polym. Chem. Ed., 6 (1964) 183.
15 K. Nakamoto, Infrared Spectra of Inorganic and Coordination Compounds, John Wiley, New York, 3rd edn., 1978, pp. 244–247.
16 T. Fujiwara and J.C. Bailar, Jr., Bull. Chem. Soc. Jpn., 61 (1988) 857.